THE INSTITUTE OF PHYSICS AND ENGINEERING IN MEDICINE

Catalogue of Diagnostic X-ray Spectra and Other Data

Produced for the
Diagnostic Radiology and Magnetic Resonance Special Interest Group
of the
Institute of Physics and Engineering in Medicine

K Cranley, B J Gilmore, G W A Fogarty and L Desponds

Report No78

Electronic Version prepared by D Sutton
September, 97

Contents

Acknowledgements

The original version of the Catalogue was published by Birch, Marshall and Ardran under the auspices of the Diagnostic Radiology Topic Group of the Hospital Physicists' Association.

A special acknowledgement of the contribution of Mr R Birch should be made, not only for his contribution to the original version of the Catalogue and the development of the spectral calculation itself, but for numerous helpful communications which also helped in preparing some related publications.

The present membership of the Diagnostic Radiology and Magnetic Resonance Special Interest Group of the Institution of Physics and Engineering in Medicine and Biology has provided encouragement and helpful suggestions.

Thanks are due to Dr R A Lerski for encouragement and to Mr A J Reilly and Dr D Sutton for preparing the Spectrum Processor.

Among the authors KC would like to acknowledge the assistance of Dr R C McGivern in fitting the photon to kerma factors and LD would like to acknowledge the contributions of Dr L Piotrowsky, Dr O Peyret and Mr R Heidsieck in the computation of the rhodium spectra.

Kieran Cranley BSc MSc PhD CPhys MInstP FIPEMB †
Brian J Gilmore BSc MSc CPhys MInstP MIPEMB ¶
George W A Fogarty BSc DPhil CPhys MInstP AMIEE §
Lionel Desponds PhD‡

†Northern Ireland Regional Medical Physics Agency, Forster Green Hospital, Belfast BT8 4HD
¶Northern Ireland Regional Medical Physics Agency, Belvoir Park Hospital, Belfast BT8 8JR
§School of Biomedical Sciences, University of Ulster at Jordanstown, BT37 0QB
‡Global X-ray Engineering, GE Medical Systems, Europe, BP 34, 78533 Buc Cedex, France

Preface

The *Catalogue of Spectral Data for Diagnostic X-Rays* (SRS-30) published in 1979 provided essential data useful for applications in diagnostic radiology and mammography. The recent availability of desk-top computing has created the opportunity for using these essential data in routine applications.

This publication is intended to include and supplement much of the spectral data in the original catalogue in a useful form on computer. The computer data are provided on compact disc (CD-ROM) and comprise a set of more than 4000 computer data files totalling about 13 Mbytes. The basic sets are of unattenuated radiographic and mammographic x-ray spectra with much wider ranges than previously provided elsewhere which can be used as input to the reader's own computer programs for attenuating as required. The Spectrum Processor program provided allows spectra to be processed and then saved for future use. Spectra from tungsten, molybdenum and rhodium targets are included.

Attenuation coefficients for various materials, photon to kerma data for some materials of dosimetric interest and data relating half value layer to total filtration are included.

A sample listing is provided, in a dialect of the Basic computer language, of a program for attenuating spectra and calculating tube outputs, mean photon energies and HVL values.

The section on data for estimating x-ray tube total filtration includes the data published in graphical form in *Data for Estimating X-Ray Tube Total Filtration* (IPSM 64) at 6 degree, 8 degree,..., 22 degree target angles, and in addition, 7 degrees, 9 degrees,..., 21 degrees.

The mammographic section includes and extends some data previously published in *Commissioning and Routine Testing of Mammographic X-ray Systems* (IPSM 59[2nd edition]).

These sets of data may be used for a wide range of applications including patient dosimetry, radiation protection and modelling of experiments, in a more accessible form than that which has been available to date.

SECTION 1

Introduction

1.1 X-ray production

X-rays are produced when a beam of electrons, thermionically emitted from an x-ray tube cathode, is accelerated by a potential difference to impinge on the target region of the anode. The enormous deceleration of the electron beam by the electrical fields around the nuclei of the target atoms results in the emission of intense x-radiation known as bremsstrahlung. The spectral distribution of x-rays produced in a thin target is approximately linear, the maximum intensity being at the minimum energy, and the minimum (vanishing) intensity being at the maximum energy of the beam of electrons. Because the depth of the point of origin of bremsstrahlung within a thick target varies, the incident electrons and the emitted x-rays are subjected to varying amounts of attenuation (filtration) by the target material.

The effect of further filtration on this energy distribution is to reduce the intensity of the lower energy x-rays much more than that of the higher energies. The resulting photon spectrum is a continuum of intensities extending over the energy range.

An additional possible process in the interaction of the electron beam with the target atoms is the creation of a vacancy in an inner orbital electronic shell. Such a vacancy can be quickly filled by electronic transition from an outer electron shell with the associated emission of an x-ray photon with characteristic energy. A multiplicity of these emissions causes discrete energy lines to be superimposed on the bremsstrahlung continuum when electrons accelerated by the x-ray tube potential have energy greater than the corresponding absorption edge energy of the target material.

In the diagnostic x-ray energy range where tungsten targets and aluminium filters are commonly used (W/Al combination), L lines are produced and depending on the tube potential, K lines may be produced. Tungsten K lines have energies at 57.97 keV (K_{α_2}), 59.31 keV (K_{α_1}), 67.23 keV (K_{β_1}) and 69.09 keV (K_{β_2}) and the L lines have energies between 8.34 keV and 11.28 keV. The tungsten target x-ray spectra of the filtered beams used in diagnostic radiology exhibit L lines at low values of filtration and K lines at tube potentials above 70 kV.

Molybdenum is commonly used as a target material in x-ray mammography in order to achieve the required radiographic contrast in the soft tissues of the female breast. These spectra are dominated by the molybdenum K line energies of 17.37 keV (K_{α_2}), 17.48 keV (K_{α_1}), 19.61 keV (K_{β_1}) and 19.96 keV (K_{β_2}). The use of molybdenum filters (Mo/Mo combination) enhances this effect by preferentially attenuating photons with energies below about 10 keV and above 20 keV.

Consideration of signal-to-noise ratio in breast imaging reveals that as compressed breast thickness increases, an advantage could be gained by increasing the energy of the spectrum. This can be achieved by replacing the molybdenum filter with rhodium or palladium or by using a rhodium target at the anode. Spectra produced using rhodium targets (Rh/Rh combination) exhibit K line energies of 20.07 keV (K_{α_2}), 20.21 keV (K_{α_1}), 22.72 keV (K_{β_1}) and 23.17 keV (K_{β_2}).

1.2 Beam quality

Beams of x-rays emerging from diagnostic x-ray tubes contain photons with a range of energies. In order to fully understand the interactions occurring within the patient and the processes leading to image production and radiation dose within the patient, a knowledge of the x-ray energy distribution is needed.

High resolution radiation detection systems capable of recording spectra are available but are used only in special circumstances and not in routine diagnostic x-ray beam monitoring.

Many other less complex means have been commonly used to describe the 'quality' of x-ray beams. The half value thickness or half value layer (HVL) is the thickness of a chosen material, usually aluminium, which reduces the radiation dose delivered by a narrow x-ray beam to 50 per cent. With a mono-energetic radiation beam, the HVL would fully describe its attenuation since the first HVL is equal to subsequent HVLs. However, diagnostic x-ray beams comprise many photon energies and therefore successive HVLs, for example, 2nd or 3rd HVL, increase with beam attenuation in low atomic number media. The lower energy components are more heavily attenuated and the beam becomes more mono-energetic with an increased average energy. The HVL alone is therefore inadequate for describing how x-rays penetrate a medium.

The kV_{peak} (kV_p) of the x-ray beam has often been quoted in addition to the (1st) HVL to describe the penetrating ability of the beam. However, while kV_p and HVL together usefully describe the properties of the x-ray beam for many purposes, the photon energy distribution (photon spectrum) or dose energy distribution (kerma spectrum) of the beam provides much more information, which is necessary for other types of calculation.

1.3 SRS-30

A theoretical method of calculating x-ray spectra which gives results in close agreement with experimental spectra has been developed by Birch and Marshall[1].

SRS-30[2] provided illustrations of the agreement between this theory and experiment.

SRS-30 provided many examples of constant potential tungsten and molybdenum target spectra calculated using this theory at voltages between 30 kV and 140 kV for various combinations of filtration, target angle and target material. Several spectra relevant to mammographic and computed tomographic (CT) applications were included and tube output and HVL values were presented for each spectrum. Exit spectra calculated for various thicknesses of soft tissue and bone were compared with incident spectra and other relevant data were presented.

1.4 Current catalogue

The purpose of this edition of the Catalogue is to provide a much wider range of x-ray photon spectra in a suitable form for a range of applications using personal computers. Unattenuated photon spectra are presented for tungsten targets at tube potential intervals in 1 kV steps from 30 kV to 150 kV and with target angles from 6 degrees to 22 degrees at one degree intervals. Tungsten target x-ray spectra are provided for tube potentials between 55 and 90 kV_p with sinusoidal waveform ripple values ranging from 0 per cent (constant potential) to 30 per cent in 5 per cent steps. Sets of data giving the relationship between HVL and total filtration are presented. Some of these data have previously been published in graphical form as IPSM 64[3].

Constant potential mammographic spectra are provided at 1 kV intervals from 25 kV to 32 kV for molybdenum target angles in steps of one degree from 9 degrees to 23 degrees. Data relating HVL and added Mo filtration for all these combinations are included for filtration of 1 mm Be, 0.03 mm Mo and 500 mm air.

Similarly, constant potential spectra for rhodium targets are provided at 1 kV intervals from 25 kV to 32 kV and for the target angle range of 9 degrees to 23 degrees in steps of one degree.

All spectra are provided at energy intervals of 0.5 keV. References to ‘target angle’ in this document imply ‘effective target angle’, unless otherwise stated. *Section 2.3* and *Appendix 1* provide discussion of these terms.

HVL information for each spectrum is not included as these values can be easily obtained by the reader using simple computing. See *section 6.5*.

Linear attenuation coefficients for a number of media and conversion factors relating photon spectra to kerma spectra for four materials of radiodiagnostic interest are provided.

CT scanners have not been specifically mentioned because of the variety of possible design parameters encountered at the present time. Nor has reference been made to the film type of penetrameter as described in SRS-30, since that method of estimating x-ray tube potential is no longer considered to be the best.

The section on commercially-used intensifying screens has also been omitted since it would not be possible to cover the range available. However, the unattenuated photon spectra provided should enable the reader to calculate photon and kerma spectra and other parameters for CT and other applications.

SECTION 2

Factors Affecting the Spectrum Shape

2.1 Tube peak kilovoltage

The peak value of the applied tube potential difference between cathode and anode determines the upper energy end point of the spectrum, whether characteristic lines occur and their relative intensities. It also affects the mean energy of the spectrum and the tube output. The output from an x-ray tube can be calculated from the area under the kerma spectrum curve and it is proportional to the peak tube potential raised to a power, depending on the amount of added filtration, which is frequently quoted as two for radiographic spectra. For mammographic spectra, this power is nearer to three[4] due to the different proportions of characteristic line and bremsstrahlung intensities combined with the K-edge filtration provided by materials such as molybdenum or rhodium.

Figures 2.1 and 2.2 illustrate the effect of varying the tube potential on some tungsten and molybdenum spectra.

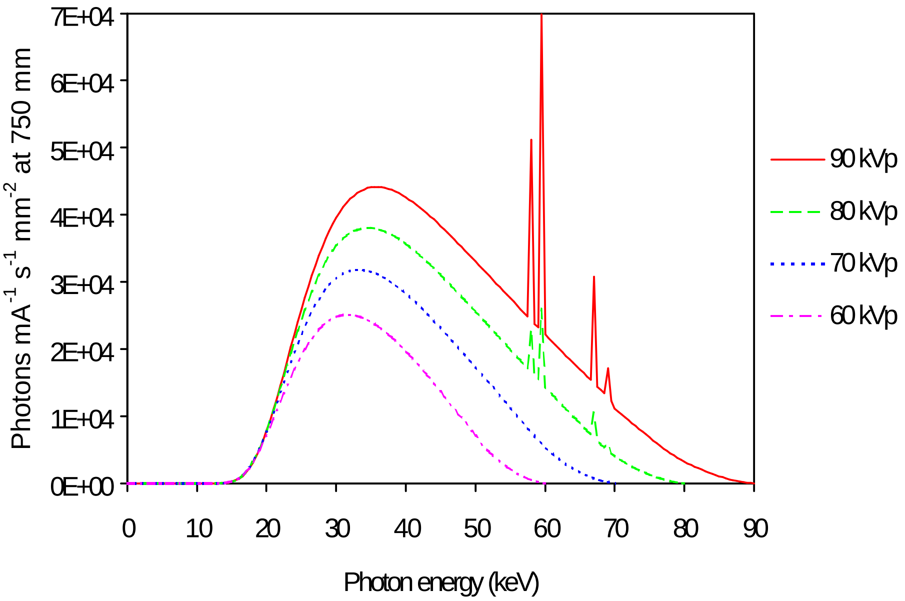

Fig 2.1 Calculated photon spectra: 12 degrees W 15% ripple, 2.5 mm Al, 750 mm air

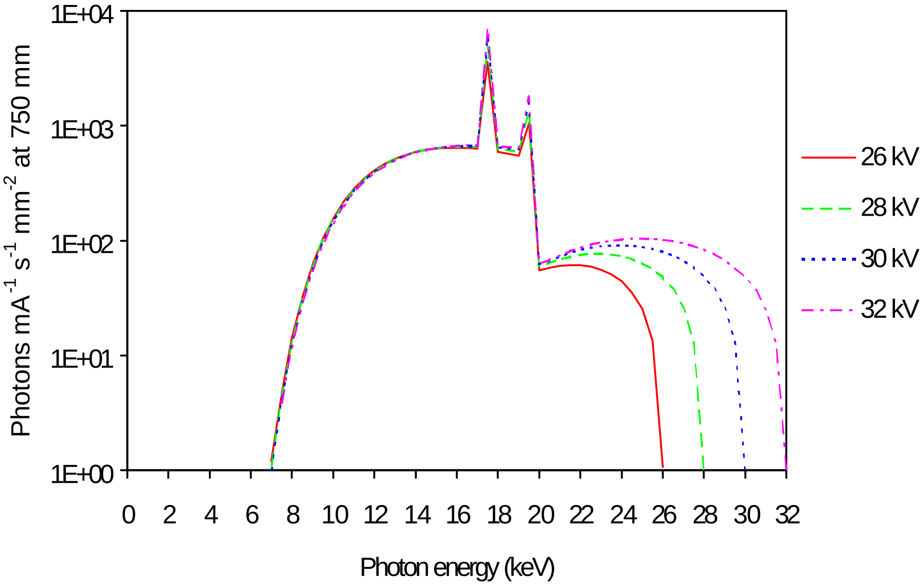

Fig 2.2 Calculated photon spectra:15 degree Mo constant potential, 1 mm Be, 0.03 mm Mo, 500 mm air

2.2 Tube potential variation during an exposure

In practice the applied tube potential may vary throughout an exposure because of a number of factors, including variations of the anode voltage due to the type of alternating mains supply, the type of rectification and the tube current. This variation is referred to as ‘ripple’ and is expressed as a percentage of the peak tube potential, defined as:

$$R = (V_{max}-V_{min})/V_{max}$$

where V_{max} and V_{min} are the maximum and minimum values of the x-ray tube potential respectively[5].

The applied tube potential for waveforms with ripple is lower than the kV_p for most of the time during an exposure. *Figure 2.3* illustrates the effect on spectral shape which is apparent mainly in the region between the peak of the continuum and the end point corresponding to the kV_p.

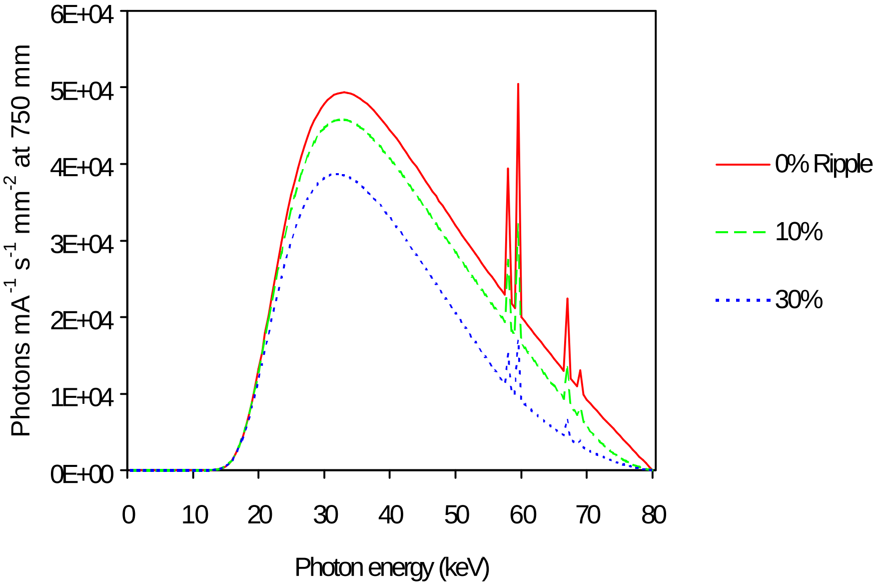

Fig 2.3 Calculated photon spectra: 80 kV 22 degrees W, 2.5 mm Al, 750 mm air

2.3 X-ray emission angle

The target angle, θ, of an x-ray tube is the angle between the electron beam and the normal to the target surface, (see *figure 2.4*). The angle chosen in the design is usually less than about 23 degrees, to allow a relatively large area of the target to be struck by the focused electron beam, and to minimise by the 'line focus principle' the focal spot area apparent to the image receptor. A small target angle is normally chosen for a very small apparent focal spot size or 'fine focus', while larger angles are used to produce 'broad focus'.

The X-ray emission angle, ψ, is the angle between the target face and the emerging x-ray beam. X-rays produced for smaller emission angles are filtered through a greater thickness of anode target material than for larger emission angles. These effects on the spectrum shape include the variation of the intensity and the energy at which the continuum peak occurs. A spectrum corresponding to a small target angle has a continuum peak at a higher energy than a spectrum from a larger target angle, (see *figure 2.5*). In many cases, as in *figure 2.4 A*, the central axis of the useful x-ray beam is along a line at 90 degrees to the electron beam. If the angle of emission is large, for example at the cathode edge of the x-ray field, less filtering occurs, but if ψ is small more filtering by the target occurs.

As ψ tends towards zero the target attenuation increases rapidly and eventually total cut-off occurs. This is known as the 'anode heel effect'. The variation in filtration also occurs in the third dimension. The result is a wide variation in both spectral shape and intensity as the point of observation changes, since all positions in the image receptor are irradiated by apparently differing shapes of focal spot.

X-ray tubes with zero target angle can be used for mammography since the x-ray field size is restricted to half of the usual diagnostic x-ray field. Advantages of this configuration include reduced extra focal radiation, square (as opposed to trapezoidal) focal spot shape and minimizing of anode wobbling in the direction of anode rotation. In the geometry in *figure 2.4 B*, the chest wall position is at the cathode side and the x-ray beam direction is confined to within the region between the 'central axis' and the tangent to the target face.

Use of geometry A to calculate spectra for x-ray tubes with zero target angle, configuration B, may give rise to the need for a small correction for emission angles between 15 and 23 degrees. This can be achieved by choosing spectra for more appropriate effective target angles, (see *Appendix 1*).

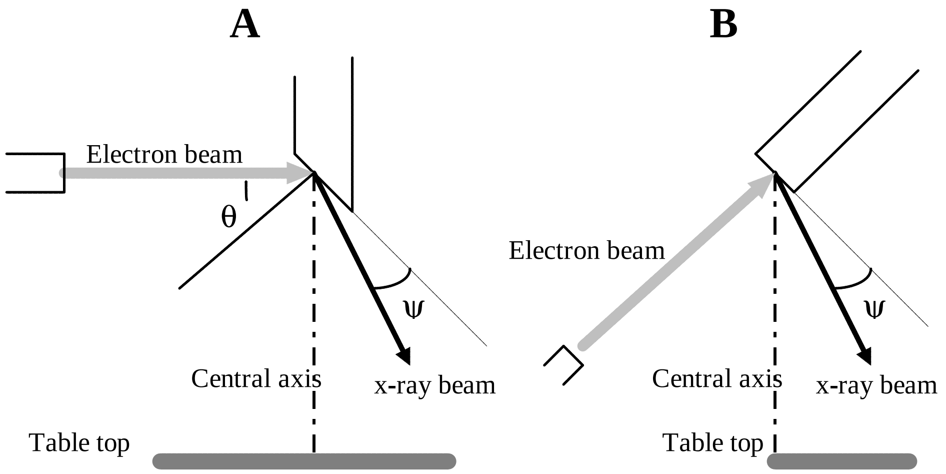

Fig 2.4 Geometry variations commonly used in x-ray tubes: θ represents the target angle and ψ is the x-ray emission angle. **A** - a radiographic arrangement; **B** - a mammographic design with a zero degree target angle.

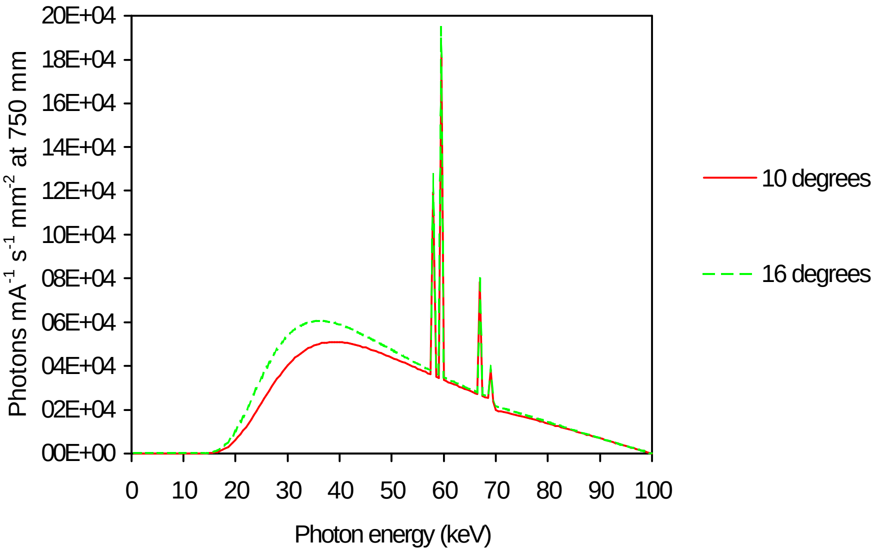

Fig 2.5 Calculated photon spectra: 100 kV W constant potential, 2.5 mm Al, 750 mm air

2.4 Filtration

Filtration of the x-ray beam along the path between the target and the patient occurs in a number of ways. The major filtration before x-rays reach the patient consists of the following possibilities:

- the target itself
- the exit window of the x-ray tube which is made from glass, metal or beryllium
- insulating oil in which the tube may be immersed
- a further layer of glass
- an added filter of aluminium, molybdenum or some other material chosen according to the energy of its K absorption edge
- a thin layer of tungsten on the inner surface of the glass envelope due to condensation of tungsten vapour arising from the filament or target
- the light beam mirror
- a plastic exit port window and
- a transmission ionisation chamber with polymethyl methacrylate walls.

In addition there is a thickness of air and possibly a compression paddle made from materials such as Lexan or polymethyl methacrylate before the x-rays reach the entrance surface of the patient.

The effect of aluminium filtration is preferential removal of photons from the lower energy side of the continuum peak of the spectrum. K edge filters can be used to modify the spectrum shape at the higher energies. Examples of rare earth K edge filtration are tungsten spectra with varying thicknesses of erbium (*figure 2.6*) and molybdenum spectra with varying molybdenum filter thicknesses (*figure 2.7*).

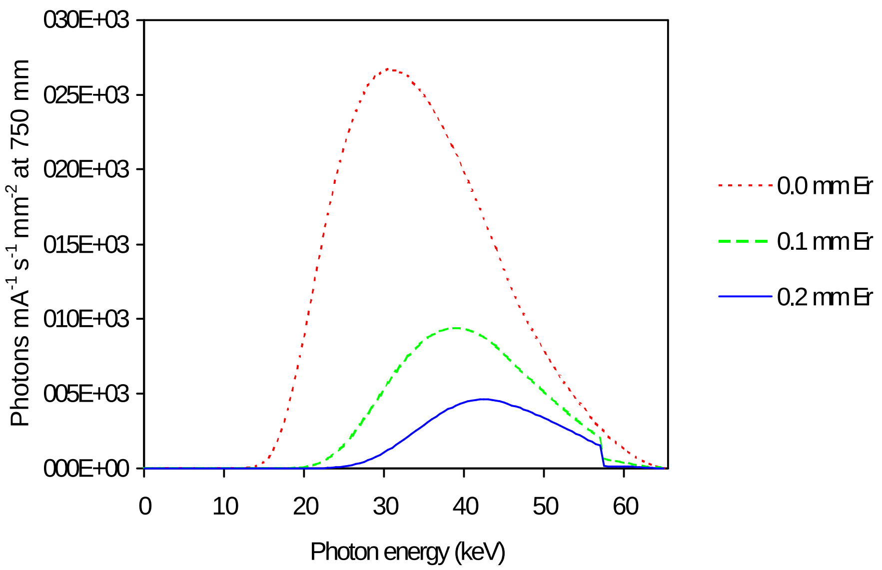

Fig 2.6 Calculated photon spectra: 65 kV 16 degrees W 30% ripple, 2.5 mm Al

2.5 Extra focal radiation

A small proportion of electrons striking the focal spot area of the target are repelled by the electrons of the target atoms and subsequently re-accelerated towards the target in the high voltage field. When these electrons re-impinge on the anode and cause the emission of bremsstrahlung, the point of origin of these x-rays can be outside the x-ray tube focus. This off-focus or extra focal radiation has low energy and intensity contributing between 5 per cent and 10 per cent of the dose[2]. The amount present in practice varies from one x-ray tube assembly design to another. However, its effect on the spectral shape is insignificant[2]. The theory of Birch and Marshall[1] includes a contribution from extra focal radiation typically present in diagnostic x-ray beams.

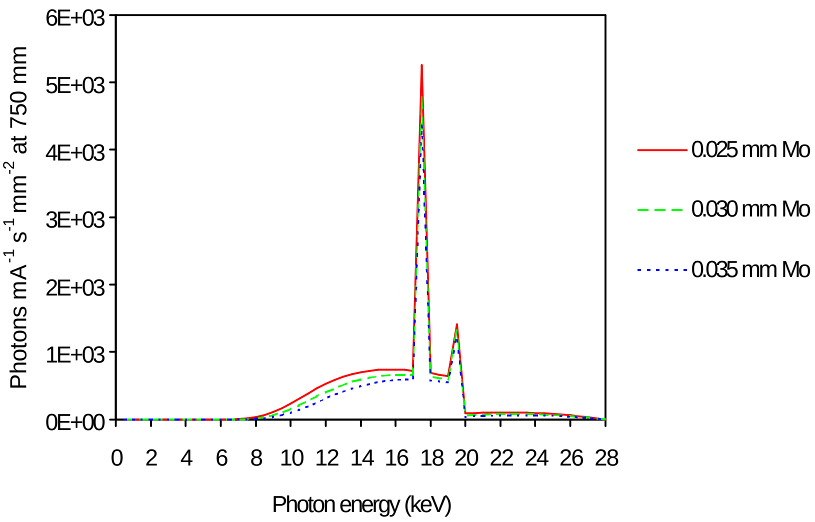

Fig 2.7 Calculated photon spectra: 28 kV 15 degrees Mo, 1 mm Be, 500 mm air

2.6 Target roughness

The surface of the target, when new, would appear to be smooth if viewed by eye. However, with prolonged use, the surface may become roughened because of localised temperature rises causing melting with subsequent pitting and the formation of other surface irregularities. This results in the introduction of multiple effective target angles and the x-rays produced at these effective target angles are subjected to an increased path length of target material. The resulting beam emitted at the range of effective target angles from a roughened surface is thus hardened. This is normally only a significant effect for ageing x-ray tubes.

SECTION 3

Calculation of Spectral Data

3.1 Radiographic photon spectra

Unattenuated constant potential photon spectra for the energy range 30 to 150 keV were calculated for 6 degree to 22 degree tungsten targets using the method of Birch and Marshall[1]. Energy steps of 0.5 keV were used for these calculations rather than 1 keV intervals which were used by Birch and Marshall. The current work makes use of XCOM[6] to calculate linear attenuation coefficients of various materials encountered. Previous calculations using this method have used fitting routines to calculate attenuation coefficients from McMaster et al[7].

3.2 Radiographic photon spectra with waveform ripple

The shape of the tube potential waveform of many multi-pulse generators can be approximated using a sinusoidal function[2,3]. The spectrum produced when the tube potential varies can be modelled by combining a number of spectra generated at different constant tube potentials, each one being weighted according to the time for which that tube potential occurs.

In computing spectra with tube potential waveform ripple, it has been assumed that the tube current is constant and not affected by tube potential waveform. By combining constant potential spectra in appropriately weighted proportions, tube potential waveforms with sinusoidal ripple varying from 0 per cent (constant potential) to 30 per cent in steps of 5 per cent were calculated for 6 degree to 22 degree tungsten targets.

The tube potential range for the data set with sinusoidal ripple was chosen as 55 kV to 90 kV to include the two reference points of 60 kV and 80 kV with upper and lower limits of approximately ±10 per cent.

3.3 Mammographic photon spectra

Molybdenum target spectra have been calculated at a narrow range of tube constant potentials from 25 to 32 kV in steps of 1 kV. The most common tube potential used in the United Kingdom for screen-film mammography is 28 kV_p, while that in the United States is 25 or 26 kV_p. The range 25 to 32 kV therefore covers most situations encountered in current practice. The target angle range of 9 to 23 degrees was chosen since this was felt to be applicable to many makes of mammographic x-ray set, 9 degrees often being close to the x-ray tube manufacturer's reference axis and 15 degrees often being close to the apparent target angle within the area of a compressed breast[8]. In calculating mammographic spectra, the geometry in *figure 2.4 A* was assumed. The relationship between target angles for this configuration and that of *figure 2.4 B* is given in *Appendix 1*.

Rhodium spectra have been calculated for the same range of tube potentials and target angles. Characteristic lines were added using a 1.63 power law[9] using the formula for characteristic line intensity described by Birch and Marshall[1]. The intensities of the characteristic lines were adjusted using x-ray spectra measured using a Ge detector from an x-ray tube with a rhodium coated track driven by a high frequency (less than 4 per cent ripple) generator. The x-ray beam was attenuated by a 25 micron thick rhodium filter. The accuracy of this adjustment procedure is estimated to be within 3 per cent for the K_α lines and within 6 per cent for the K_β lines. Attenuation coefficients for rhodium for this part of the calculation were taken from Storm and Israel[10] which agree with those of XCOM[6] within -0.4 per cent at 5 keV to +1.6 per cent at 15 keV. *Figure 3.1* illustrates a rhodium spectrum.

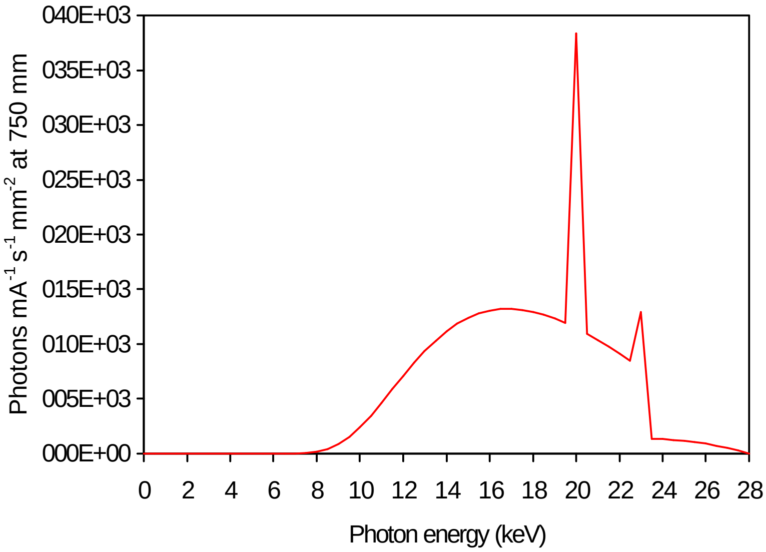

Fig 3.1 Calculated photon spectrum: 28 kV 22.5 degrees Rh constant potential, 0.8 mm Be, 0.025 mm Rh, 350 mm air

3.4 Photon to kerma data

Kerma in air is the kinetic energy transferred to ionising particles per unit mass of air by indirectly ionising radiation. No correction is required for bremsstrahlung produced by the ionising particles as this is negligible at photon energies below about 1 MeV.

Photon spectra can be converted to kerma in air spectra using the photon to kerma in air conversion factors provided. These conversion factors were calculated using the values of mass-energy absorption coefficients[11] for air as defined by ICRU[12] by applying polynomial fitting routines to the logarithms of the data. Minimal residuals of the fits were found for 4th order fitting of the data from 4 to 20 keV, 4th order from 20 to 80 keV and quadratic fit from 80 to 150 keV. Conversion factors for adipose tissue[12], skeletal muscle[12] and cortical bone[12] were determined using the same procedure.

SECTION 4

Calculation of Data for Estimating Tube Total Filtration

The HVL method can be used to determine the total filtration of diagnostic x-ray tubes with an accuracy of ±10 per cent[13] provided the HVL can be measured within ±0.06 mm Al, the kV_p within ±1.9 kV, tube potential ripple within ±5 per cent and the effective target angle is known within ±1.8 degrees. This assumes the availability of accurate data relating HVL to tube total filtration as described below.

4.1 Radiographic data

Theoretical tungsten target spectra with various tube potential waveforms were subjected to attenuation by 750 mm of air and a range of thicknesses of aluminium from 0.5 mm to 4 mm. The output value and HVL were computed for each filter combination using photon to kerma in air conversion factors. This enabled the relationship between HVL and total filtration to be determined for each set of spectral conditions.

IPSM 64[3] presented theoretical HVL-total filtration data for the range of tungsten target angles from 6 degrees to 22 degrees in steps of 2 degrees, peak tube potentials in the range 55 to 90 kV in steps of 5 kV, and ripple values of tube potential waveform from 0 to 30 per cent in steps of 5 per cent. The data provided here supplement IPSM 64[3] by providing a 1 degree increment in target angle.

Illustrations of verification and use of these data were provided and information was presented on the use of the HVL method to determine total filtration. An assessment of errors in the result was also provided[3,13].

Following measurements of the HVL, the peak tube potential and the tube potential ripple of an x-ray beam, the total filtration of the x-ray tube can be determined using the corresponding HVL-total filtration data appropriate to the target angle of the x-ray tube. Data representing the relationship between HVL and total filtration for ranges of tube potentials, tube potential ripple and target angles appropriate to the particular x-ray set are used for the estimate of total filtration. For target angles, tube potential or ripple values falling between those presented the total filtration may be interpolated accurately. *Figure 4.1* shows an example of the relationship between HVL and *total* filtration for W/Al systems.

Figure 4.2 illustrates the range of HVL values due to different target angles at a particular tube potential and total filtration value.

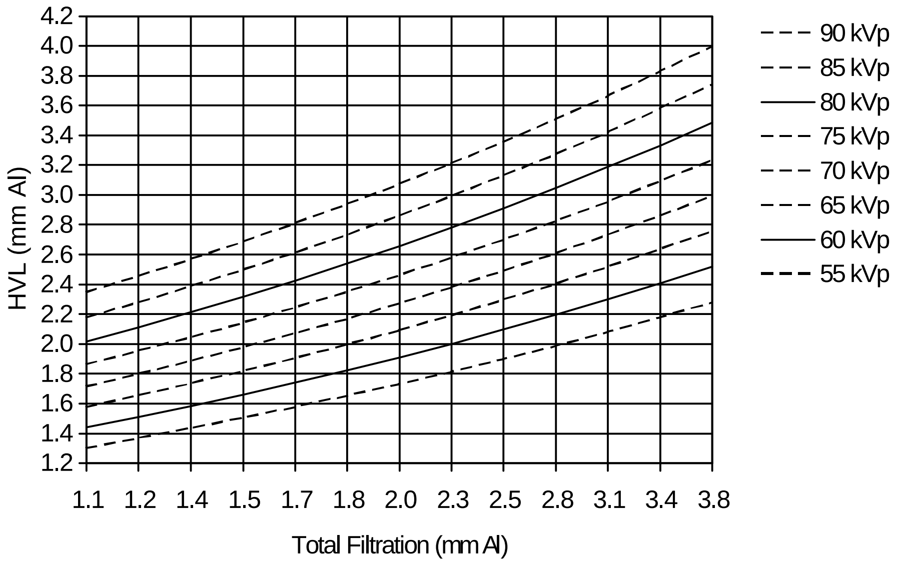

Fig 4.1 From tungsten spectra: Target angle 6 degrees, 30% ripple, 750 mm air

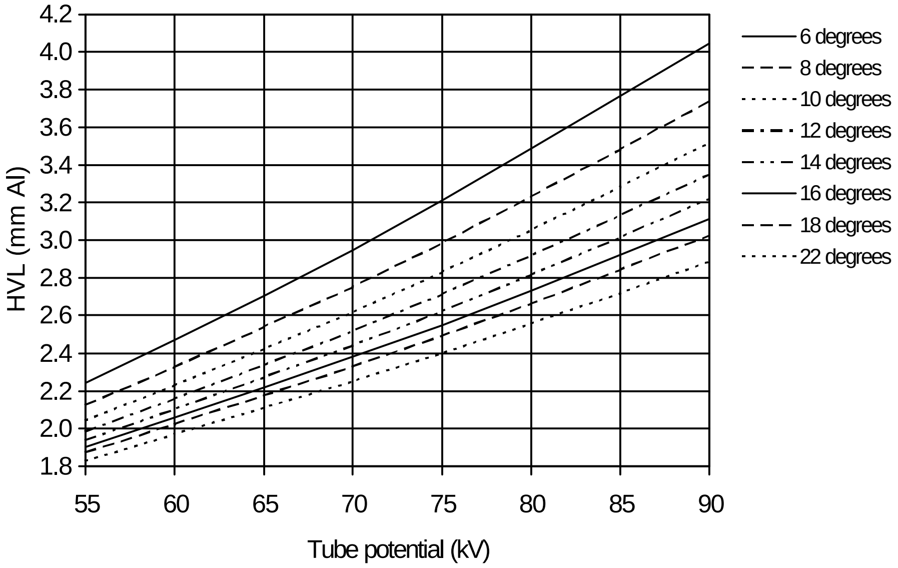

Fig 4.2 From tungsten spectra: Constant potential, total filtration 2.5 mm Al, 750 mm air

4.2 Mammographic data

Theoretical molybdenum constant potential spectra were attenuated by 1 mm beryllium, 500 mm air and a range of molybdenum thicknesses from 0.015 mm to 0.045 mm. The output was determined and the HVL values were computed for each spectrum and Mo filter thickness. This enabled the calculation of HVL-total filtration data for each set of spectral conditions.

Further sets of data (not included here) were obtained[14] by attenuating the above molybdenum target spectra with a range of thicknesses of breast compression plate, each time calculating the HVL in aluminium equivalent thickness. This allowed data sets to be constructed which relate HVL to thickness of *added* molybdenum filter. Thus a measurement of HVL, in the presence of various thicknesses of polymethyl methacrylate compression plate, and use of these sets of data, can lead to an accurate determination of molybdenum filter thickness[8, 14].

Figure 4.3 shows an example of the relationship between HVL and added filtration for Mo/Mo systems, in this case, where a 2 mm thick compression paddle is used to support the aluminium filters.

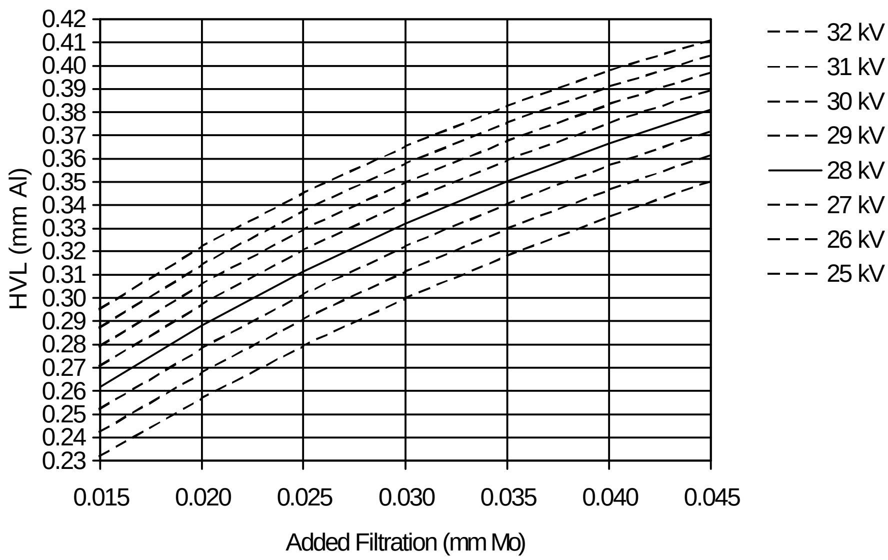

Fig 4.3 From molybdenum spectra: Target angle 15 degrees, constant potential, 1 mm Be, 500 mm air, 2 mm polymethyl methacrylate compression plate.

SECTION 5

Comparison of Current Data with SRS-30

5.1 Calculated constant potential spectra

Calculated constant potential 17 degree, 10 degree and 22 degree tungsten spectra are compared in *figures 5.1 to 5.9* with those given in the previous Catalogue[2]. A comparison of 17 degree molybdenum spectra is given in *figure 5.10*. The examples illustrated confirm that there is good agreement between the current and the SRS-30 spectra, despite the differences between the old and new attenuation coefficients discussed in *section 5.2*. The reader is referred to *section 5.4* for a comparison of output and HVL data.

The 30 kV, 17 degree tungsten spectra in *figure 5.1* demonstrate characteristic L lines. The currently used 0.5 keV interval for tungsten spectra displays better energy resolution of K lines in *figures 5.4, 5.5, 5.6* and *5.8* than the SRS-30 spectra which have 1.0 keV energy intervals.

.

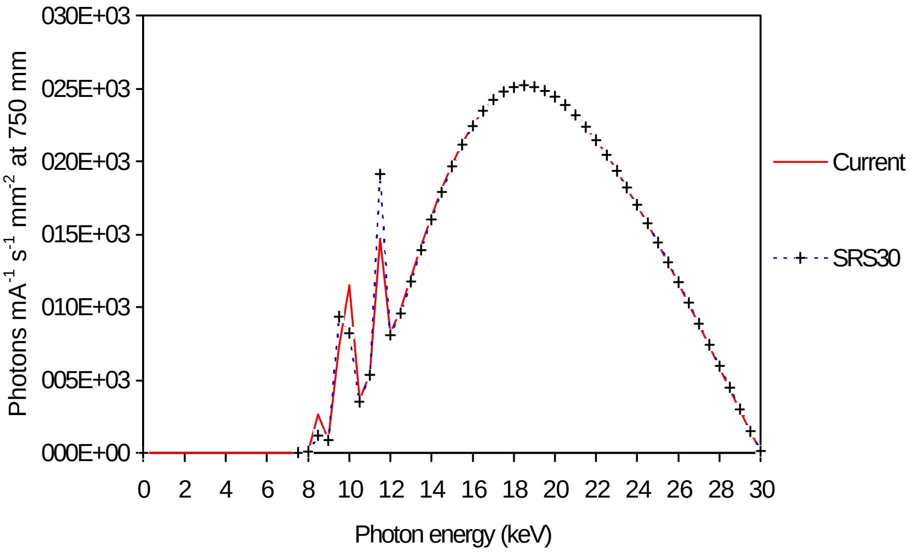

Fig 5.1 Calculated photon spectra: 30 kV 17 degrees W constant potential, 1.0 mm Be, 0.5 mm Al, 350 mm air

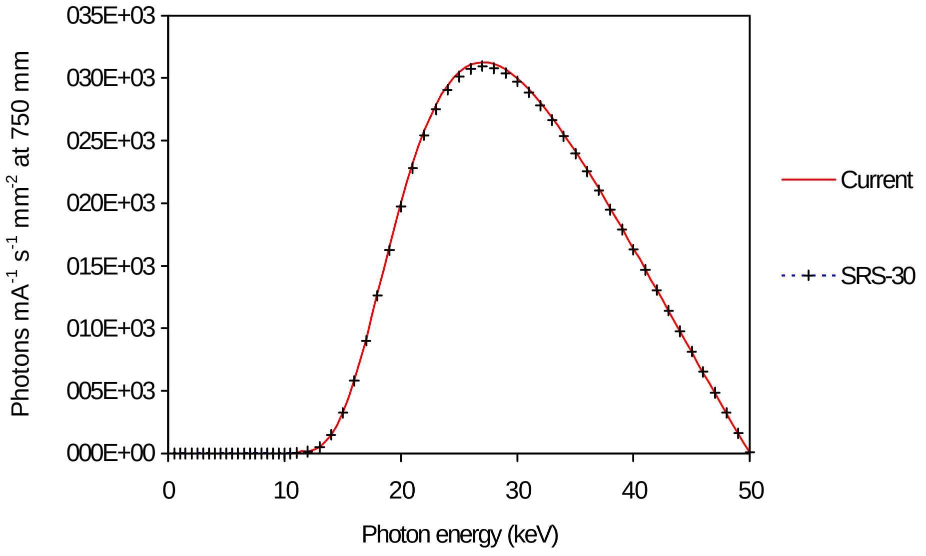

Fig 5.2 Calculated photon spectra: 50 kV 17 degrees W constant potential, 1.5 mm Al, 750 mm air

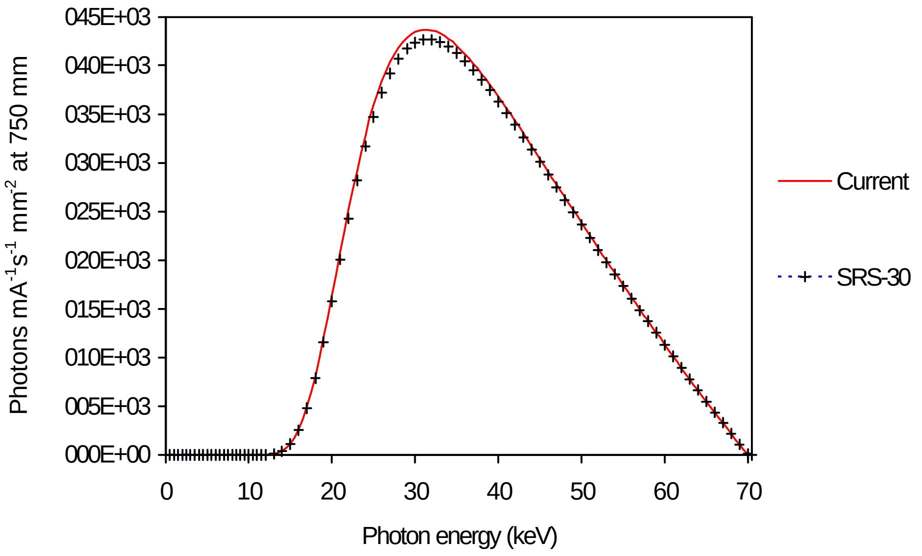

Fig 5.3 Calculated photon spectra: 70 kV 17 degrees W constant potential, 2.0 mm Al, 750 mm air

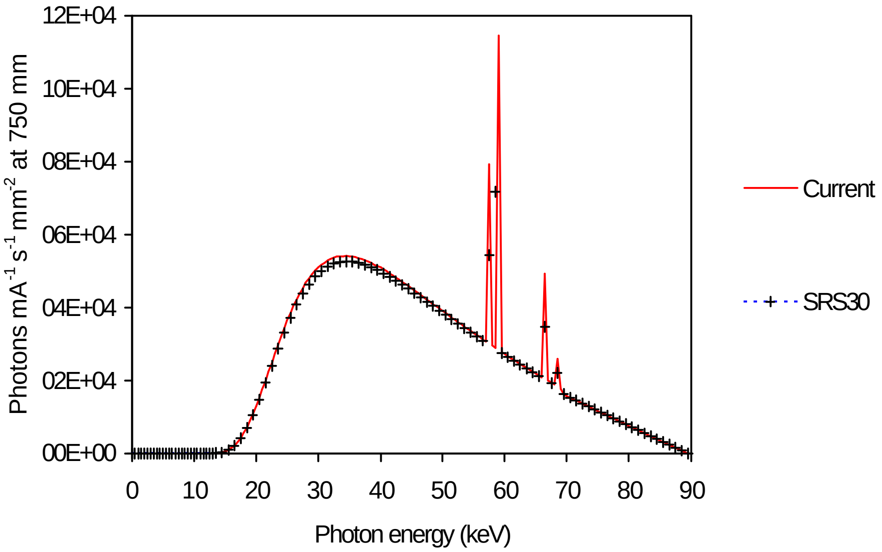

Fig 5.4 Calculated photon spectra: 90 kV 17 degrees W constant potential, 2.5 mm Al, 750 mm air

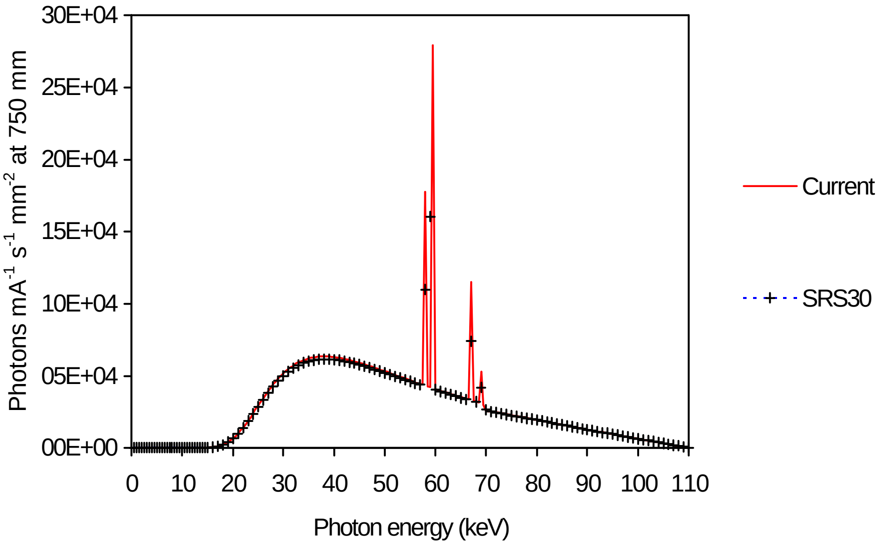

Fig 5.5 Calculated photon spectra: 110 kV 17 degrees W constant potential, 3.0 mm Al, 750 mm air

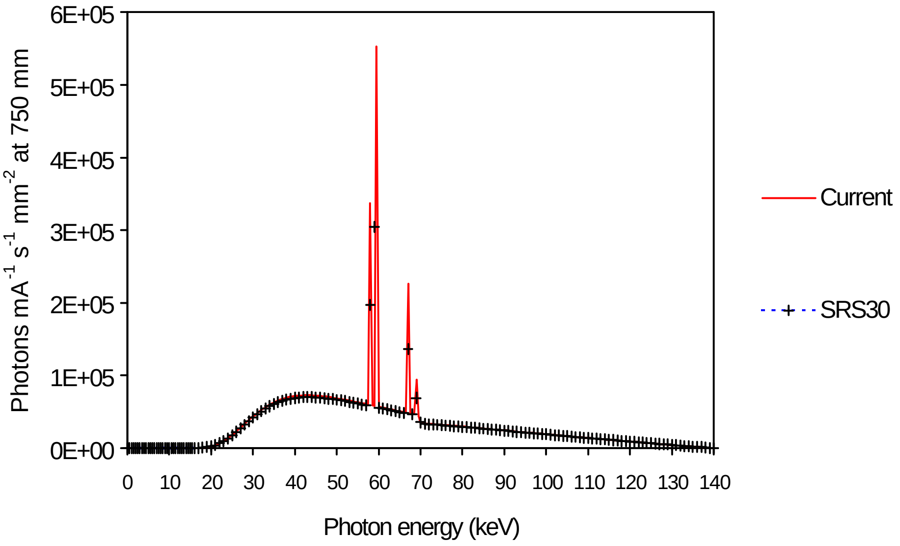

Fig 5.6 Calculated photon spectra: 140 kV 17 degrees W constant potential, 4.0 mm Al, 750 mm air

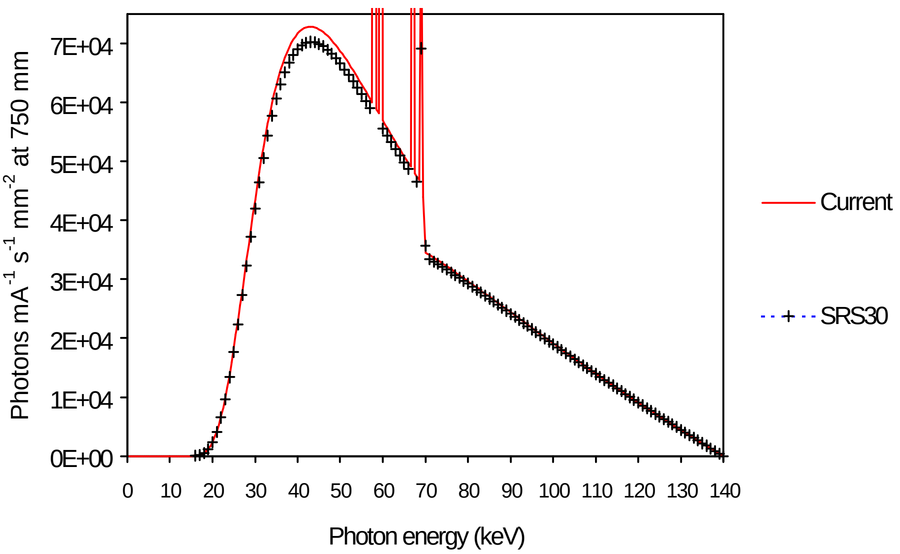

Fig 5.7 Calculated photon spectra: 140 kV 17 degrees W constant potential, 4.0 mm Al, 750 mm air. Same data as in previous figure, but with K-lines truncated to enable a closer comparison of the continuum.

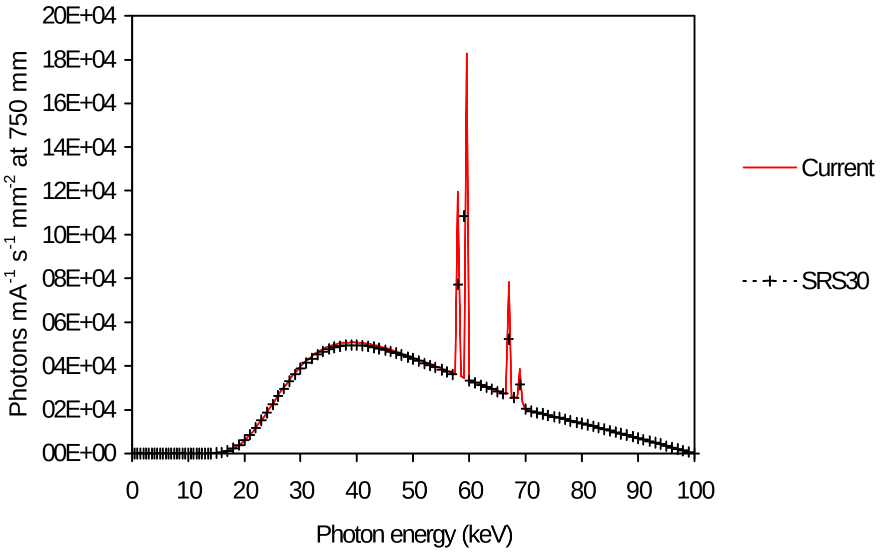

Fig 5.8 Calculated photon spectra: 100 kV 10 degrees W constant potential, 2.5 mm Al, 750 mm air

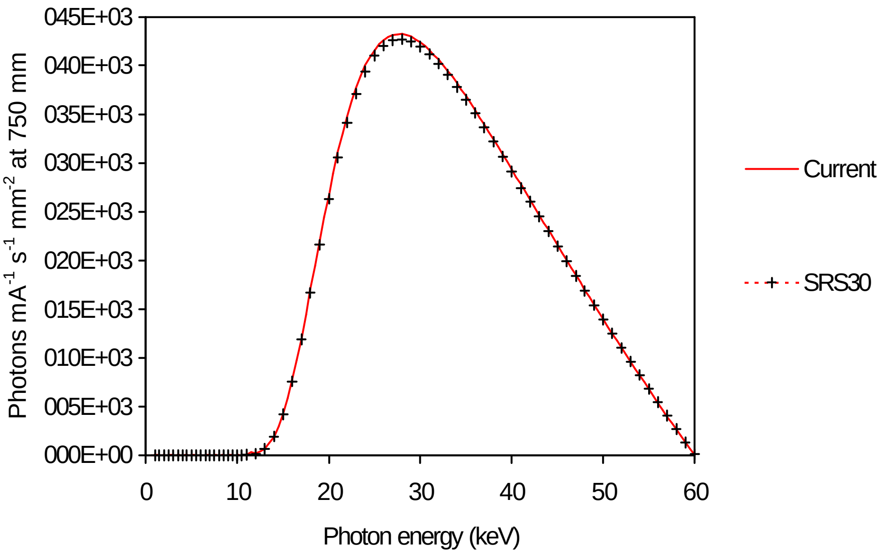

Fig 5.9 Calculated photon spectra: 60 kV 22 degrees W constant potential, 1.5 mm Al, 750 mm air

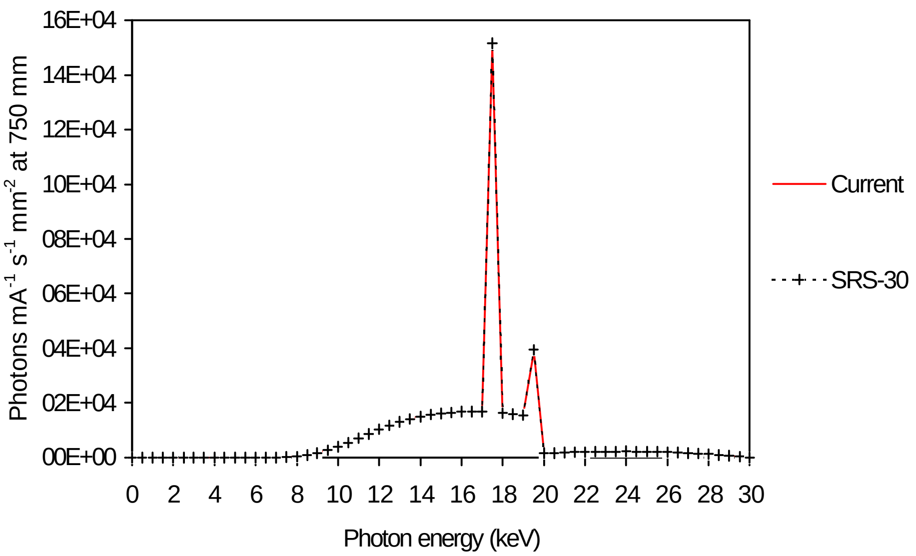

Fig 5.10 Calculated photon spectra: 30 kV 17 degrees Mo constant potential, 1.0 mm Be, 0.03 mm Mo, 350 mm air

5.2 Attenuation coefficients

The new linear attenuation coefficients (Berger and Hubbell[6]) of several materials have been compared with those of McMaster et al[7] used in SRS-30.

Comparisons over the energy range 10 keV to 150 keV reveal agreement for tungsten within 4.0 per cent, molybdenum within 1.5 per cent, aluminium within 2.5 per cent and copper within 3.5 per cent, while significant differences are apparent for beryllium within 12 per cent, air (see *figure 5.11*) within 8 per cent and polymethyl methacrylate within 20 per cent compared with Perspex.

Other compound materials presented have the advantage of a traceable composition. For example, 'air' as defined by ICRU-44[12] refers to dry air near sea level, but the substance previously described[2] by that name had not been defined.

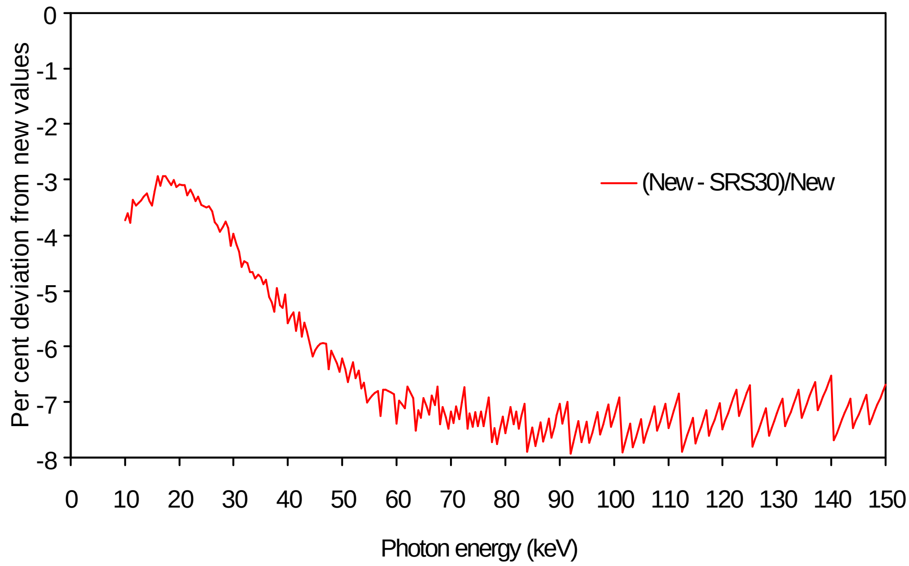

Fig 5.11 Deviations of the SRS-30 values from the new values of linear attenuation coefficients for air

5.3 Photon to kerma conversion factors

Figures 5.12 and 5.13 show comparisons between the new values of conversion factors for ICRU-44[12] air, ICRU-44[12] adipose tissue and ICRU-44[12] skeletal muscle and the SRS-30 values for 'air' and 'tissue'. There are small but significant differences between the old and the new values. *Figure 5.14* includes the conversion factors for ICRU-44[12] cortical bone.

5.4 HVL and tube output data

The validity of the current theoretical HVL values has been assessed by comparisons with SRS-30[2] for target angles of 17 degrees (*table 5.1*) and 10 degrees and 22 degrees (*table 5.2*). Tube outputs are compared in *tables 5.3 and 5.4*.

HVL values for the current data are in good agreement, typically within -1.4 per cent (-0.4 per cent to -2.2 per cent), while the current output values are typically over-estimated by +9.9 per cent (+8.7 per cent to +10.9 per cent) when compared with those in SRS-30.

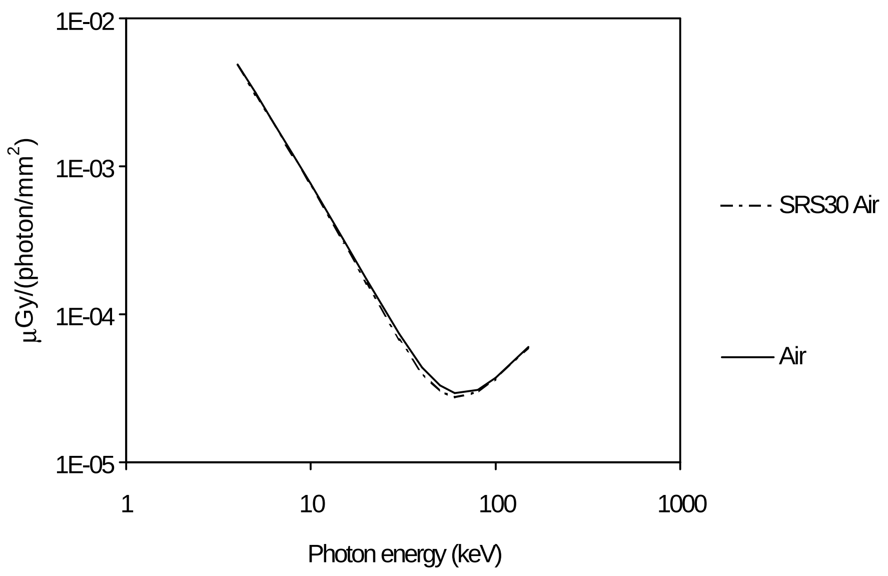

Fig 5.12 Comparison of photon to kerma conversion factors.

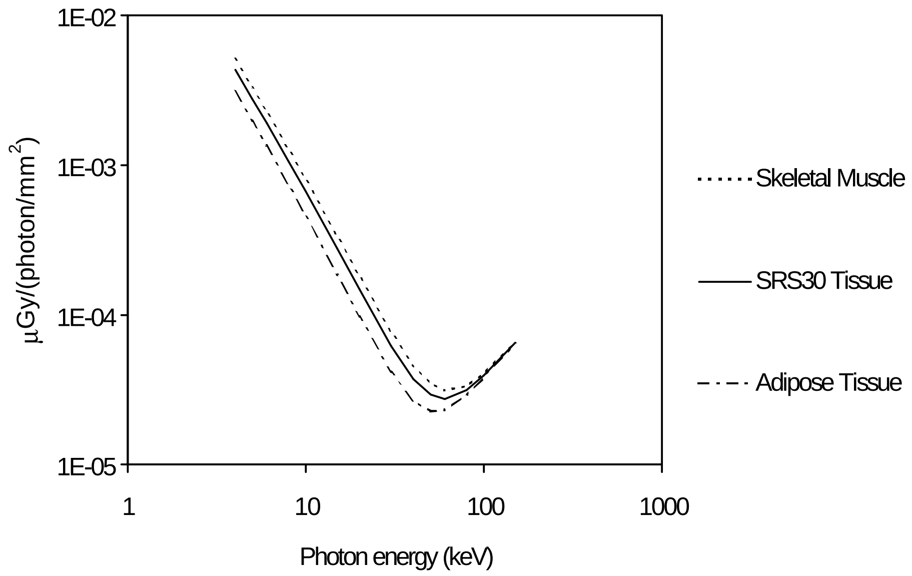

Fig 5.13 Comparison of photon to kerma conversion factors.

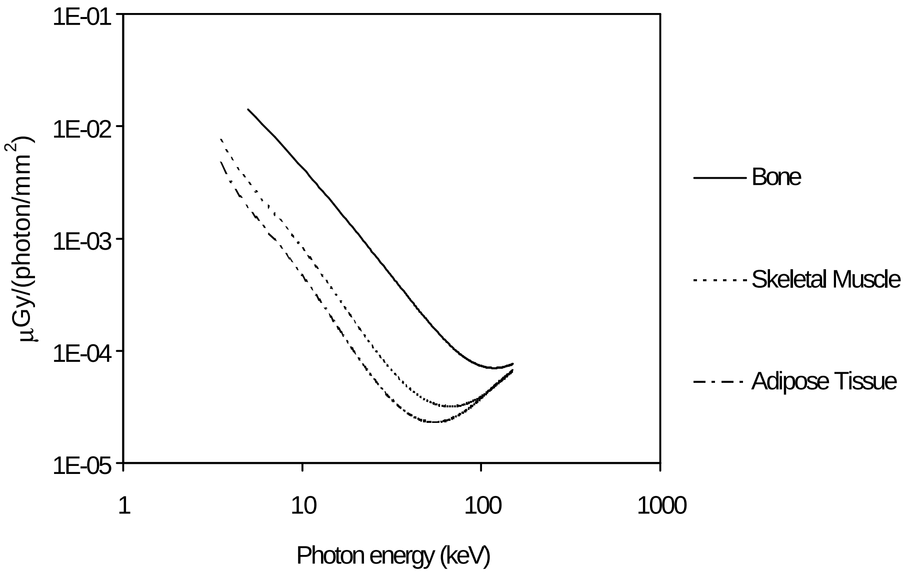

Fig 5.14 Comparison of photon to kerma conversion factors.

The new kerma in air conversion factors are the main cause of the 10 per cent differences in outputs. Further explanation of these differences lies in the fact that up-to-date attenuation coefficients have been used in the calculations, which should give more accurate results. Additional confirmation has been provided by the comparisons with experimental spectra and other data given in IPSM 64[3].

Table 5.5 compares the current theoretical data with theoretical and experimental data given for 22 degree tungsten targets in SRS-30. The current data give good agreement for HVL values within 1.2 per cent (-0.3 per cent to +2.7 per cent) and for tube output values within 4.6 per cent (+0.8 per cent to +6.1 per cent) when compared with SRS-30 theoretical data for 'additional' filter thicknesses in the range 2 to 4 mm Al. For additional filters of 1 mm Al, the current HVL values are +4.6 per cent (+4.0 per cent to +5.3 per cent), while tube outputs are within 1.1 per cent (-1.8 per cent to +3.6 per cent). Added filtration values between 2 mm and 4 mm Al are typical of the diagnostic range and filtrations of 1 mm Al would not normally be found. Similar agreement is found with the experimental values quoted in SRS-30.

The small differences in the current calculated HVL and tube output values may be explained by the differences in attenuation coefficients of beryllium, air and polymethyl methacrylate and photon to kerma in air conversion factors.

It is concluded that the current theoretical spectra are in satisfactory agreement with those of SRS-30 in view of the stated agreement between spectral shapes, output values and HVL data.

Table 5.1 Comparison of HVL values (mm Al) calculated by Birch et al[2] and present work [in brackets]. Constant potential waveform, 17° W target.

kV	Total filtration mm Al 1.5	2.0	2.5	3.0	4.0
50	1.31[1.31]	1.54[1.53]	1.74[1.73]		
60	1.55[1.54]	1.83[1.81]	2.07[2.05]		
70	1.79[1.78]	2.11[2.08]	2.38[2.36]		
80		2.42[2.39]	2.74[2.70]	3.03[2.98]	
90		2.76[2.72]	3.11[3.07]	3.43[3.38]	
100		3.12[3.07]	3.50[3.44]	3.85[3.78]	4.46[4.38]
110			3.90[3.83]	4.27[4.19]	4.91[4.82]
120			4.31[4.23]	4.69[4.60]	5.35[5.26]
140			5.15[5.04]	5.55[5.43]	6.23[6.10]

Table 5.2 Comparison of HVL values (mm Al) calculated by Birch et al[2] and present work [in brackets]. Constant potential waveform, 10° and 22° W targets.

kV	Total filtration mm Al	Target angle 10°	22°
60	1.5	1.75[1.73]	1.48[1.46]
100	2.5	4.05[3.98]	3.28[3.23]
140	2.5	5.97[5.84]	4.78[4.67]

Table 5.3 Comparison of output values in μGy $mA^{-1}s^{-1}$ at 750 mm calculated by Birch et al[2] and present work [in brackets]. Constant potential waveform, 17° W target.

kV	Total filtration mm Al 1.5	2.0	2.5	3.0	4.0
50	112.9[122.9]	83.8[91.1]	65.0[70.7]		
60	153.6[169.8]	118.5[130.7]	95.1[104.7]		
70	193.9[214.7]	153.9[170.0]	126.4[139.5]		
80		190.5[211.2]	159.8[176.9]	137.0[151.4]	
90		230.1[254.1]	196.4[216.6]	170.9[188.2]	
100		270.5[298.3]	234.3[258.0]	206.5[227.1]	166.2[182.2]
110			273.9[300.9]	244.0[267.7]	199.9[218.7]
120			315.0[345.0]	283.2[309.8]	235.7[257.1]
140			399.9[437.3]	365.1[398.7]	311.5[339.2]

Table 5.4 Comparison of output values in μGy $mA^{-1}s^{-1}$ at 750 mm calculated by Birch et al[2] and present work [in brackets]. Constant potential waveform, 10° and 22° W targets.

kV	Total filtration mm Al	Target angle 10°	22°
60	1.5	124.3[137.7]	167.2[184.6]
100	2.5	188.4[207.1]	256.6[282.7]
140	2.5	312.9[341.3]	444.0[486.2]

Table 5.5 Comparison of calculated HVL and output values with theoretical and experimental values quoted in SRS-30[2]. Constant potential waveform, 22° W target.

Tube kV	Additional filter* mm Al	HVL mm Al Current Theory	HVL mm Al SRS-30 Theory	HVL mm Al Experiment	Exposure rate μGy $mA^{-1}s^{-1}$ at 0.75 m Current Theory	Exposure rate μGy $mA^{-1}s^{-1}$ at 0.75 m SRS-30 Theory	Exposure rate μGy $mA^{-1}s^{-1}$ at 0.75 m Experiment
50	1.0	1.20	1.14	1.14	116.7	119.0	121.8
60	1.0	1.40	1.33	1.31	161.8	161.1	156.6
80	1.0	1.82	1.75	1.75	249.9	243.5	241.9
100	1.0	2.34	2.25	2.21	340.6	329.5	356.7
50	2.0	1.64	1.60	1.62	64.2	63.9	63.5
60	2.0	1.93	1.88	1.87	95.6	93.0	87.0
80	2.0	2.50	2.45	2.48	163.1	156.2	147.9
100	2.0	3.16	3.11	3.11	239.6	228.4	233.2
100	4.0	4.42	4.42	4.47	148.3	140.3	139.2
120	4.0	5.27	5.27	5.20	214.2	202.5	208.8
140	4.0	6.08	6.10	5.95	287.9	271.7	278.4

***In addition to 2 m air, 3 mm Be and 4.7 mm polymethyl methacrylate

SECTION 6

Presentation of Data

6.1 Photon spectra

Table 6.1 gives a summary of the photon spectrum file names provided. For constant potential spectra, the file extension is '.SPC' and for spectra with voltage ripple, the extension is '.R05' for 5 per cent ripple, 'R10' for 10 per cent ripple, and so on. Photon spectra are presented as the variation with energy of *photons per mAs per mm^2 at 750 mm.*

The format of each file type should be examined in detail. The kV_p value ascribed to a spectrum, as given in the title line within each set of spectral data, represents the maximum voltage applied to the tube to generate the spectrum. This title line contains a string, composed of the kV_p followed by 'K', the target angle followed by a 'D0', the target material, either 'W' for tungsten, 'M' for molybdenum or 'R' for rhodium. The last character is a '2' which indicates that there are two energy intervals per keV. For example, '031K09D0R2' describes a 31 kV, 9 degree, rhodium spectrum at 0.5 keV intervals, which is unfiltered. An asterisk is added to this by the attenuation program to indicate that the spectrum has been processed by the program.

The remaining lines give firstly the energy in keV, followed by the photon spectrum value, separated by a space.

Table 6.1 Photon spectrum file names

 # # #$.EXT**

### kV_p range	** ** Target angle(^{o})	**$** Target material	**EXT** Kilovoltage ripple
###=030 - 150 (1 kV intervals)	** = 06 - 22 (1^o intervals)	$ = 0 Tungsten	EXT = SPC ie constant potential
###=055 - 090 (5 kV intervals)	** = 06 - 22 (1^o intervals)	$ = 0 Tungsten	EXT = R05 - R30 ie 5% to 30%
###=025 - 032 (1 kV intervals)	** = 09 - 23 (1^o intervals)	$ = 1 Molybdenum	EXT = SPC ie constant potential
###=025 - 032 (1 kV intervals)	** = 09 - 23 (1^o intervals)	$ = 2 Rhodium	EXT = SPC ie constant potential

6.2 Attenuation coefficients

The data files representing attenuation coefficients calculated by XCOM[6] are given in *table 6.2*. These files are in the form of comma-separated data pairs, the energy first in 0.5 keV intervals from 0.5 keV to 150 keV, followed by the linear attenuation coefficient in units of mm^{-1}.

6.3 Photon to kerma data

Photon to kerma conversion factors are included on CD-ROM in four files, ‘kermair.csv’ for air, ‘kermadp.csv’ for adipose tissue, ‘kermskm.csv’ for skeletal muscle and ‘kermbne.csv’ for bone. The data in these files are in comma separated pairs with energy intervals of 0.5 keV, followed by the values in $\mu Gy\ photon^{-1}\ mm^2$.

To convert the photon spectra to kerma in air data, the photon to kerma in air file should be used. Similarly, to convert a photon spectrum into kerma in adipose tissue (ICRU-44[12]), skeletal muscle (ICRU-44[12]) or cortical bone (ICRU-44[12]) the appropriate file should be employed.

Table 6.2 Disc file names for linear attenuation coefficients of various materials

Material	File name
adipose tissue [ICRU 44]	adipose.csv
air (dry, near sea level)	air.csv
aluminium	al.csv
barium	ba.csv
beryllium	be.csv
bone (cortical [ICRU 44])	bone.csv
calcium	ca.csv
copper	cu.csv
erbium	er.csv
gallium	ga.csv
glass (borosilicate [Pyrex])	glass.csv
gold	au.csv
hafnium	hf.csv
iodine	i.csv
iron	fe.csv
lead	pb.csv
magnesium	mg.csv
manganese	mn.csv
molybdenum	mo.csv
muscle (skeletal [ICRU 44])	skeletal.csv
niobium	nb.csv
palladium	pd.csv
platinum	pt.csv
polymethyl methacrylate	pmm.csv
rhodium	rh.csv
silicon	si.csv
tissue (soft [ICRU-44])	tiss.csv
titanium	ti.csv
tungsten	w.csv
water (liquid H_2O)	wat.csv
yttrium	y.csv
zinc	zn.csv

6.4 HVL - total filtration data

Tables 6.3 and *6.4* summarise how the CD ROM tungsten and molybdenum file names are coded.

Table 6.3 HVL-total filtration file names (tungsten targets only)

 # # # $ **@@.EXT

kV_p range	Target angle (°)	Ripple	EXT	Comment
###=055 - 090 (+5 kV intervals)	$* = 06 - 22 (1° intervals)	*@=0% or *@@=05% - 30%	EXT = HVL	Contain mm, µGy/mAs, mean energy & HVL
###$=9055 (-5 kV intervals)	** = 06 - 22 (1° intervals)		Ripple EXT = R00 - R30 (0% - 30%) in 5% steps	Contain a summary of HVL values

The files '055060%.HVL' through '0902230%.HVL' give, after the descriptor code line indicating kV_p, target angle and ripple value, a title line with headings 'mm Al', 'µGy per mAs', 'Mean Energy keV' and 'HVL mm Al'. The following lines give values corresponding to these titles for total filtration values from 0.54 mm Al to 6.94 mm Al..

The file names '905506.R00' to '905522.R30' refer to the range of kV_ps from 90 to 55 in steps of -5 kV, the target angle, for example 6 degrees to 22 degrees, and ripple values of zero to 30 per cent. These files contain a descriptor line which confirms target angle and ripple value, followed by nine columns of numbers. The first column gives values of total filtration, from 0.54 mm Al to 6.94 mm Al, and the next column gives the HVL values in mm Al corresponding to 90 kV_p, calculated by including 750 mm air and the corresponding thickness of aluminium. The next column gives the data for 85 kV_p, and so on to 55 kV_p in the last column.

Files with file names 055060.R05 to 090060.R05 give 55 to 90 kV, 6 degree target angle, 5 per cent ripple spectra while 090170.R15 gives 90 kV, 17 degree target angle, 15 per cent ripple data. 0750810%.HVL represents HVL values at 75 kV, 8 degree target angle and 10 per cent ripple.

The data in this set of files, when plotted, give graphs similar to those in IPSM 64[3]. The files beginning with ‘9055...’ bring together HVL data for the various kV_ps by providing a summary of HVL versus filtration data.

Table 6.4 summarises the ‘.HVL’ files related to the mammographic spectra.

Table 6.4 HVL-total filtration file names (molybdenum targets only)

 # # DEG.HVL

## Target angle range (^{o})	Comment
## = 09 - 23 (1^o intervals)	Contain µGy/mAs, mean energy & HVL (mm Al) kV = 32 - 25 Filtration: 1 mm Be, 500 mm air, 0.015 - 0.045 mm Mo

Each of these includes data relating to eight spectra from 25 kV to 32 kV. These have been attenuated firstly by 500 mm air and then by seven values of added Mo filtration from 0.015 mm to 0.045 mm, which are listed with output values, mean energies and HVL values in mm Al.

6.5 Sample computer program for attenuating spectra

The program ‘A10u8.bas’ is provided as a listing in the Appendix 2. The program has been written in a dialect of the Basic language which can easily be translated into other formats. A compiled version of the program ‘A10u8.exe’ is also provided with the data. This may be run by entering the program name, without extension.

This program listing is given as an example only and will undoubtedly need to be tailored to suit the reader’s own needs.

Appendix 1 Relationship between effective target angle and x-ray emission angle

The calculation of the x-ray spectra[1] for a target angle *q* is based on the assumption that the useful x-rays emerge at 90 degrees to the electron beam and at angle *q* to the target surface, (see *figure A1 A*). Hence when the x-rays emerge at any other angle, ψ, it is necessary to substitute an 'effective target angle' *e* for the actual target angle, *q*.

The electron beam can be considered to penetrate into the target up to a penetration depth *p* and the x-rays generated at this depth which leave the target along the beam centre-line are subjected to filtration by a thickness *f* of the target material. If *q* is the target angle (ie the angle between the normal to the target surface and the electron beam direction), then

$$\tan q = \frac{p}{f} \qquad \textit{(A.1)}$$

X-rays which emerge at any other angle ψ to the target surface, (see *figure A1 B*), are subject to filtration by a thickness SE of the target material given by

$$\mathrm{SE} = \frac{\mathrm{p}\cos\theta}{\sin\psi} \qquad (\mathrm{A.2})$$

For an x-ray to emerge at 90 degrees to the electron beam and to be filtered by the same thickness SE, the target angle of the tube would have to be *e*, where *e* is given by:-

$$\varepsilon = \tan^{-1}\left[\frac{\sin\psi}{\cos\theta}\right] \qquad (\mathrm{A.3})$$

Thus *e* may be described as the 'effective target angle' for the beam which emerges at an angle ψ to the target surface. When the beam emerges at an angle ψ=*q* to the target surface the effective target angle is *q*.

In the case of zero target angle (see *figure A1 C*), the electrons strike the target surface at normal incidence. If the x-rays emerge at an angle ξ to the electron beam and are subject to filtration by a thickness *f* of the target material, then

$$\cos\xi = \frac{\mathrm{p}}{\mathrm{f}} \qquad (\mathrm{A.4})$$

The same amount of filtration would be encountered in a 'conventional' x-ray set with target angle e_0 where

$$\varepsilon_0 = \tan^{-1}[\cos\xi] \quad (A.5)$$

It is noted that $\xi + \psi = 90$ degrees and so $\cos \xi = \sin \psi$ and hence

$$\varepsilon_0 = \tan^{-1}[\sin\psi] \quad (A.6)$$

e_0 may be described as the 'effective target angle' for the beam which emerges at angle ψ to the target surface. Note that equation (A.6) is a special case of equation (A.3) since in zero target angle mammographic tubes $q = 0$ and hence $\cos q = 1$.

The relationship between the effective target angle, e_0 and x-ray emission angle, ψ, for zero target angle x-ray tubes is given in *Table A.1*

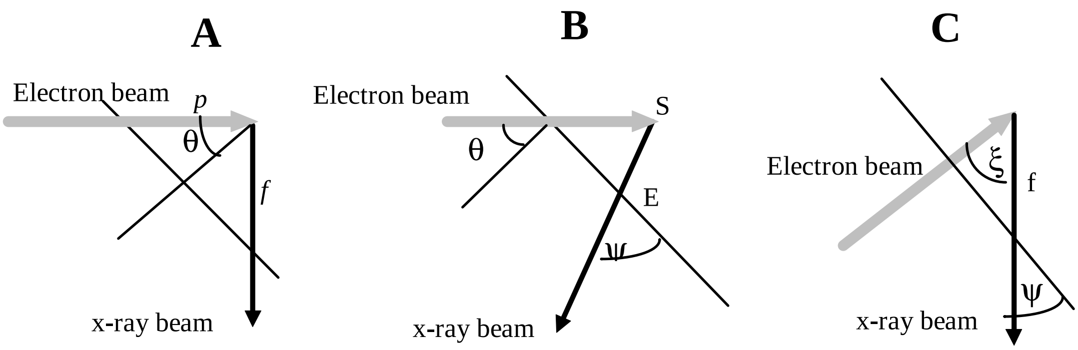

Fig A1 Penetration of the electron beam into the target

.

Table A.1 Relationship between effective target angle, e_0 and x-ray emission angle, ψ for zero target angle x-ray tubes

e_0,, degrees	ψ, degrees
9	8.9
11	10.8
13	12.7
15	14.5
17	16.3
19	18.0
21	19.7
23	21.3

Appendix 2 Sample attenuation program listing

```
REM                        PROGRAM A10u8
REM This program reads a spectrum file, attenuates it with a specified number of filters,
REM and computes the tube output, mean photon energy and HVL of the filtered
REM spectrum
        INPUT "FILESPEC ",F$
        OPEN F$ FOR INPUT AS #1
        INPUT #1,C$
1       A$=LEFT$(C$,3)
        KVP=VAL(A$)
        PRINT USING "###";KVP;
        PRINT " kVp ";
        PRINT USING "\\";MID$(C$,5,2);
        PRINT " Degrees ";
        PRINT USING "\ \";RIGHT$(C$,3);
        PRINT " Ripple"
        ANGLE=VAL(MID$(C$,5,2))
2       DIM VAT(300),YS(300),EN(300),ATT$(20),TMM(20),YF(300),KERMA(300)
        IF MID$(C$,10,1)="2" THEN PRINT " INTERVAL = 0.5 keV"
        DE=0.5
        NOINT%=KVP/DE
                        FOR I=1 TO NOINT%
                        YS(I)=0:YF(I)=0:EN(I)=0
                        NEXT I
                FOR I=1 TO NOINT%
                INPUT #1,EN(I),YS(I)
                NEXT I
        CLOSE #1
        INPUT " Input the no of attenuators ",NOATT
        FOR I=1 TO NOATT
                PRINT " Attenuator no. ";I;
                INPUT ATT$(I)
                INPUT " Thickness (mm) ",TMM(I)
                OPEN ATT$(I)+".CSV" FOR INPUT AS #I
                        PRINT ATT$(I)
                        FOR J=1 TO NOINT%
                        INPUT #I, EN(J),VAT(J)
                        IF VAT(J)*TMM(I) >1410 THEN YS(I)=0:GOTO 3
                        YS(J) = YS(J)*EXP(-VAT(J)*TMM(I))
3                       NEXT J
                CLOSE #I
                NEXT I
        PRINT " No. of FILTERS: ";NOATT
                INPUT "Output filespec ",O$
        OPEN O$ FOR OUTPUT AS #3
                PRINT #3,C$+"*"
                        FOR I=1 TO NOINT%
                        PRINT #3, using "####.#";EN(I);
```

```
                    PRINT #3, " ";
                    PRINT #3, using "#.#####^^^^"; YS(I)
                    NEXT I
                    FOR I=1 TO NOINT%
                    YF(I)=YS(I)
                    NEXT I
        CLOSE #3
        PRINT "Please wait ..."
        OPEN "KERMAIR.CSV" FOR INPUT AS #4
                FOR I=1 TO 300
                INPUT #4, EN(I), KERMA(I)
                NEXT I
        CLOSE #4
        OPEN "AL.CSV" FOR INPUT AS #5
                FOR I=1 TO NOINT%
                INPUT #5, EN(I),VAT(I)
                NEXT I
        CLOSE #5
        KX=0:HVL=0:TT=0:TLO=0:OPUT=0:ENERGY=0
                            REM Calculate the mean photon energy
4       TQT1=0:TQT2=0:TQT3=0
        KX=KX+1
                FOR L=1 TO NOINT%
                TQT1=TQT1+YF(L)*KERMA(L)
                TQT2=TQT2+YF(L)*DE*L
                TQT3=TQT3+YF(L)
                NEXT L
        IF KX=1 THEN 5
        GOTO 6
5       OPUT=TQT1
        ENERGY=TQT2/TQT3
        THI=20.0
        GOTO 7
6       IF TQT1>(OPUT/2) THEN TLO=TT ELSE THI=TT
        IF TQT1<(OPUT/2)*1.000005 AND TQT1>(OPUT/2)*0.999995 THEN 9
7       HVL=(THI+TLO)/2
        TT=HVL
                FOR I=1 TO NOINT%
                IF VAT(I)*TT > 1410 THEN YF(I)=0:GOTO 8
                YF(I)=YS(I)*EXP(-VAT(I)*TT)
8               NEXT I
        GOTO 4
9               PRINT USING "##########.###";OPUT;
                PRINT " uGy per mAs at 750 mm in air.":PRINT "  Mean energy = ";
                PRINT USING "###.#";ENERGY;:PRINT "keV. HVL = ";
                PRINT USING "##.######";HVL;:PRINT " mm Al";
10              PRINT "Finished  "
        END
```

References

1 Birch R and Marshall M 1979 Computation of Bremsstrahlung X-ray Spectra and Comparison with Spectra Measured with a Ge(Li) Detector *Phys Med Biol* **24** 505-517

2 Birch R, Marshall M and Ardran G M 1979 *Catalogue of Spectral Data for Diagnostic X-Rays* Hospital Physicists' Association Scientific Report Series 30 (IPSM, PO Box 303 York)

3 Cranley K, Gilmore B J and Fogarty G W A 1991 *Data for Estimating X-Ray Tube Total Filtration* Institute of Physical Sciences in Medicine Report No 64 (IPSM, PO Box 303 York)

4 Harpen M D 1996 A Mathematical Spread Sheet Application for Production of Entrance Skin Exposure Nomograms *Med Phys* **23(2)** 241-242

5 International Electrotechnical Commission 1984 *Medical Radiology - Terminology* IEC 788 (IEC, Geneva)

6 Berger M J and Hubbell J H 1987 *XCOM: Photon Cross Sections on a Personal Computer* US Department of Commerce NBSIR 87-3597

7 McMaster W H, Kerr Del Grande N, Mallett J H and Hubbell J H 1969 *Compilation of X-ray Cross Sections* UCRL Report 50174, Section II, Rev 1 (University of California, Livermore)

8 Cranley K 1991 Measuring the Filtration of Mammographic X-Ray Tubes with Molybdenum Targets *Brit J Radiol* **64** 842-845

9 Green M and Cosslett V E 1968 Measurements of K, L and M Shell X-ray Production Efficiencies *Brit J Appl Phys (J Phys D),* **1**, 425-436

10 Storm E and Israel H 1970 *Photon Cross Sections from 1 keV to 100 MeV for Elements Z=1 to Z=100* Nuclear Data Tables A7, 565-581 (Academic Press)

11 Hubbell J H and Seltzer S M 1995 *Tables of X-Ray Mass Attenuation Coefficients and Mass-Energy Absorption Coefficients 1 keV to 20 MeV for Elements Z=1 to 92 and 48 Additional Substances of Dosimetric Interest* US Department of Commerce NISTIR 5632

12 ICRU 1989 *Tissue Substitutes in Radiation Dosimetry and Measurement* Report 44. International Commission on Radiation Units and Measurements. Bethesda, MD

13 Gilmore B J and Cranley K 1990 Errors in the Determination of Total Filtration of Diagnostic X-Ray Tubes by the HVL Method *Phys Med Biol* **35** 999-1015

14 Law J, Dance D R, Faulkner K, Fitzgerald M C, Ramsdale M L and Robinson A 1994 *Commissioning and Routine Testing of Mammographic X-Ray Systems* IPSM Report No 59, 2nd Edition (IPSM PO Box 303 York)